ELSEVIER

Journal of Alloys and Compounds 408–412 (2006) 248–252

Journal of ALLOYS AND COMPOUNDS

www.elsevier.com/locate/jallcom

Local structure of molten $LaCl_3$ analyzed by X-ray diffraction and La–L_{III} absorption-edge XAFS technique

Y. Iwadate [a,*], K. Suzuki [a], N. Onda [b], K. Fukushima [b], S. Watanabe [c], H. Matsuura [c], A. Kajinami [d], K. Takase [e], N. Ohtori [e], N. Umesaki [f], H. Kofuji [g], M. Myochin [g]

[a] *Graduate School of Science and Technology, Chiba University, Inage-ku, Chiba 263-8522, Japan*
[b] *Department of Applied Chemistry and Biotechnology, Chiba University, Inage-ku, Chiba 263-8522, Japan*
[c] *Research Laboratory for Nuclear Reactors, Tokyo Institute of Technology, O-okayama, Meguro-ku, Tokyo 152-8550, Japan*
[d] *Faculty of Engineering, Kobe University, Rokkodai, Nada-ku, Kobe 657-8501, Japan*
[e] *Graduate School of Science and Technology, Niigata University, Igarashi-Ninocho, Niigata 950-2181, Japan*
[f] *Japan Synchrotron Radiation Research Institute, Mikazuki, Hyogo 679-5198, Japan*
[g] *Japan Nuclear Cycle Development Institute, Tokai-mura, Ibaraki 319-1194, Japan*

Available online 2 June 2005

Abstract

From the radial distribution analysis of X-ray diffraction, the nearest neighbor La–Cl distance and coordination number of Cl around La in molten $LaCl_3$ were estimated to be about 0.28 nm and nearly equal to 6, respectively. On the other hand, according to the XAFS measurements, the coordination number of Cl around La was evaluated at about 7. As a result, the local structure of molten $LaCl_3$ was thought to be described as an octahedral-like coordination scheme where La was surrounded by about six or seven Cl's. This finding led to the formation of octahedral complex ion, $LaCl_6^{3-}$, which was in agreement with results of Raman spectroscopy by other authors. The La–La distance was evaluated at about 0.5 nm from the position of a weak and broad second peak in the correlation function $g(r)$, suggesting that a distorted corner-sharing connection of two octahedral complex species was predominant in the melt.

Keywords: Local structure; Molten salt; $LaCl_3$; X-ray diffraction; XAFS

1. Introduction

In order to develop a novel processing of spent nuclear fuels, a lot of continuous efforts have been made from the technological standpoints. Much attention has been recently focused on a pyro-reprocessing of oxide fuels in molten salts with special composition and combination to make UO_2^{2+} and PuO_2^{2+} ions coexist stably. However, many scientific problems remain unsolved so as to establish this technique [1,2]. As a preliminary part of the fundamental works to put the processing into effect, the local structure of a $LaCl_3$ melt instead of UO_2^{2+} and/or PuO_2^{2+}-containing melts was analyzed by X-ray diffraction (XRD) and La–L_{III} absorption-edge XAFS technique.

The local structure of molten pure rare-earth trichlorides MCl_3 (M = Y, La–Ho) has been modeled after an octahedral coordination $(MCl_6)^{3-}$, being supported by results of Raman spectroscopy [3–5] and diffraction [6–9]. In the Raman studies, vibration modes corresponding to the octahedral coordination was observed for some rare-earth trichloride melts. In the diffraction studies, the coordination number (CN) of the first M–Cl correlation was evaluated to be about 6 for the pure melts. However, another structural image has been recently proposed in neutron diffraction (ND) and molecular dynamics (MD) works. Wasse and Salmon [10,11] reported from systematic ND studies of molten rare-earth trichlorides that the CN of the first M–Cl correlation was not always fixed at 6; for example, that of molten $LaCl_3$ was 8.2. Hutchinson et al. [12,13] obtained MD simulation results of some rare-earth trichloride melts by using a polarizable ionic model (PIM), which reproduced well the ND results by Wasse and Salmon.

* Corresponding author. Tel.: +81 43 290 3433; fax: +81 43 290 3888.
E-mail address: iwadate@faculty.chiba-u.jp (Y. Iwadate).

0925-8388/$ – see front matter © 2005 Elsevier B.V. All rights reserved.
doi:10.1016/j.jallcom.2005.04.037

The CN was simulated to be 7.9 for molten $LaCl_3$. These ND and MD works concluded that the CN changes with cation size in the pure melts. In any event, the present work was carried out so as to study what structures were formed in rare-earth trichloride melts according to two different experimental techniques, XRD and XAFS.

2. Experimental

Hygroscopic $LaCl_3$ was prepared at 650 K according to the below reaction,

$$La_2O_3 + 6NH_4Cl \rightarrow 2LaCl_3 + 6NH_3 + 3H_2O$$

After chlorination, sublimation at 1300 K for 8 h was carried out to remove impurities such as oxide and oxychlorides as well as to purify the crude $LaCl_3$. The purified sample was sealed in a thin quartz tube cell to prevent spoilage.

High temperature XRD measurements were made at 1173 K. An X-ray diffractometer in θ–θ type reflection geometry was used with Mo Kα radiation. The Q-range was $9.3\,\mathrm{nm}^{-1} \leqq Q \leqq 150\,\mathrm{nm}^{-1}$ in which 2θ is the scattering angle and $Q = 4\pi \sin\theta/\lambda$, with λ equal to 0.071069 nm. Scattered X-ray intensities were corrected for background, polarization, absorption and Compton scattering, and normalized to the coherent scattering intensity. Atomic scattering and Compton scattering factors were taken from references [14,15].

XAFS measurements were performed at the BL-7C beam line in High Energy Accelerator Research Organization (KEK) at Tsukuba, Japan. The operating energy and ring current were 2.5 GeV and 300–450 mA, respectively. The synchrotron radiation was monochromatized by double Si (1 1 1) crystals. XAFS measurement of the La–L_{III} edge for $LaCl_3$ was impossible by using the quartz cell. The edge energy $E_0 = 5.48$ keV of the La–L_{III} edge is too low to obtain sufficient intensity of transmission X-ray. Thus, the procedure proposed by Matsuura et al. [16] was applied to this work, and a disk sample was used in which the halide was scattered homogeneously in a boron nitride (BN) matrix. Since the La–L_{III} edge is close to the La–L_{III} edge for lighter lanthanides, the maximum k in the La–L_{III} edge XAFS measurement is usually limited up to about 80–90 nm^{-1}. The multielectron excitation [17] due to $2p4d \rightarrow 5d^2$ transition is not negligible for the La–L_{III} edge of lighter lanthanides. The effect usually appeared as a projection around more than $k = 56\,\mathrm{nm}^{-1}$ in the XAFS function. Thus, XAFS experiments were performed in the range of $25.0\,\mathrm{nm}^{-1} \leqq k \leqq 54.6\,\mathrm{nm}^{-1}$. Step-scanning measurements for 1 s at a datum point were performed to obtain X-ray absorption spectra.

The computer program code WinXAS ver. 2.3 developed by Ressler [18] was used to analyze the XAFS data. The FEFF8 code [19] was used to simulate the XAFS (including phase shift and backscattering amplitude). Coordination number N_j, interionic distance r_j and Debye–Waller factor σ_j^2 are obtained from the curve fitting in R-space. In the present work, the cumulant expansion technique [20] was used to treat anharmonic vibration effect. Data analysis procedure for high-temperature molten salts was summarized in [21,22]. The analytical procedure is the same as the work by Okamoto et al. [23].

3. Results and discussion

3.1. X-ray diffraction

The analytical functions used in this work are described briefly as follows. The interference function $Q \cdot i(Q)$ and pair-correlation function $g(r)$ are defined by Eqs. (1) and (2), respectively,

$$Q \cdot i(Q) = Q \cdot \frac{[I_{eu}^{coh}(Q) - \sum_i f_i(Q)^2]}{(\sum_i f_i(Q))^2} \quad (1)$$

$$g(r) = 1 + (2\pi^2 r\rho_0)^{-1} \times \int_0^{Q_{max}} Q \cdot i(Q)\, \sin(Qr)\, \mathrm{d}Q \quad (2)$$

where $f_i(Q)$ is the atomic scattering factor, ρ_0 the average number density, $I_{eu}^{coh}(Q)$ the total coherent intensity function, and Q_{max} is the maximum value of Q for the scattering experiment. The analytical procedures were almost identical to those of Narten [24].

Fig. 1 shows three pair-correlation functions, $g(r)$'s. One is calculated from the original intensity data and the other two are corrected in the tail-ends of the coherent intensity $i(Q)$ as illustrated in Fig. 2, where the original $i(Q)$ in the range of $Q \geqq 130\,\mathrm{nm}^{-1}$ is multiplied by 1/3 (correction 1) and 1/10 (correction 2), respectively, in order not to affect the first CN. The noise in $g(r)$ is eliminated by these corrections. It can be seen that the typical peaks appeared at about $r = 0.28$ and 0.5 nm, the slight shoulder around $r = 0.4$ nm. The first

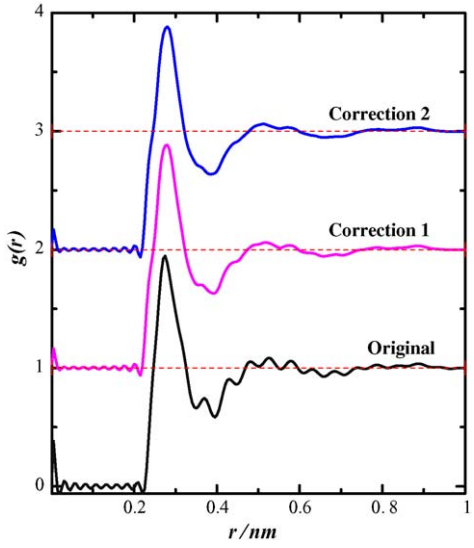

Fig. 1. Pair-correlation functions $g(r)$ of molten $LaCl_3$ at 1173 K.

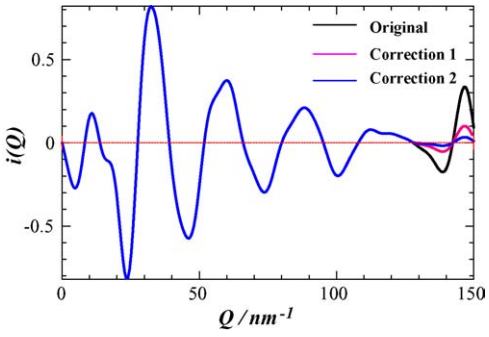

Fig. 2. Coherent scattering intensity $i(Q)$ of molten $LaCl_3$. The original $i(Q)$ in the range of $Q \geqq 130\,nm^{-1}$ is multiplied by 1/3 (correction 1) and 1/10 (correction 2), respectively.

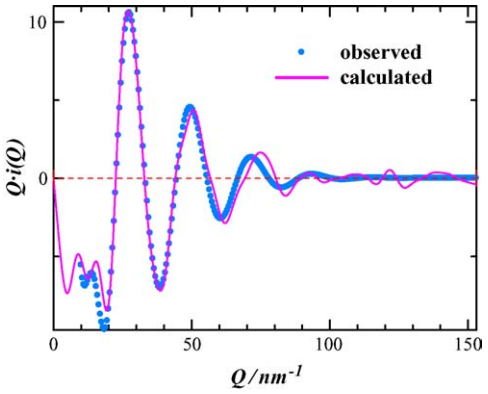

Fig. 3. Interference function $Q \cdot i(Q)$ of molten $LaCl_3$.

peaks in $g(r)$ are thought to be due to the nearest neighbor La–Cl correlation, and then Cl–Cl and La–La with increasing r. Since the intensities of the first peaks are not much greater than those of the first minima just behind the peaks, the first coordination shells might not be stabilized very much. This implies the existence of some distinct or short-lived local geometry.

For a better understanding of the melt structure, the structural parameters for each atomic pair are needed to be refined by the correlation method in the (Q, $Q \cdot i(Q)$) space, using a non-linear least squares fitting of Eq. (3),

$$Q \cdot i(Q) = \frac{[\sum_i \sum_j n_{ij} f_i(Q) f_j(Q) \times \exp(-b_{ij} Q^2)\ \sin(Q r_{ij})/r_{ij}]}{(\sum_i f_i(Q))^2} \quad (3)$$

where n_{ij}, r_{ij}, and b_{ij} are the average coordination number, the average interatomic distance, and the temperature factor for the atomic pair i–j, respectively. Each atomic pair was presumed to be Gaussian-distributed, centered at r_{ij} with a mean square displacement $2b_{ij}$. The initial values of the structural parameters on fitting were preset to be equal to the parameters obtained in the $g(r)$ analysis. Tentative assignments of the atomic pairs were at first made by consulting the ionic radii by Shannon [25], the crystallographic data [26] and the results for molten $LaCl_3$ [23]. The structural parameters within the relatively short range, for example, for the La–Cl pair, were calculated from the interference function $Q \cdot i(Q)$ data for the large Q region. As for the other Cl–Cl and La–La correlations, the $Q \cdot i(Q)$ data over the whole range of measurements were available. As depicted in Fig. 3, the observed $Q \cdot i(Q)$'s were well reproduced by the least squares fitted parameters for molten $LaCl_3$ listed in Table 1. The statistical errors in n_{ij}, r_{ij}, b_{ij}, and $\left\langle \Delta r_{ij}^2 \right\rangle^{1/2}$ were estimated to be about ±0.2, ±0.001 nm, $\pm 0.5 \times 10^{-6}\,nm^2$, and ±0.001 nm, respectively, where $\left\langle \Delta r_{ij}^2 \right\rangle^{1/2}$ is defined by $(2b_{ij})^{1/2}$. The coordination number of the nearest neighbor La–Cl pair was estimated at about 6.20 and the atomic distances of the La–Cl and Cl–Cl pairs were 0.282 and 0.412 nm for both melts, respectively. The atomic distance ratio of $r_{Cl–Cl}/r_{La–Cl}$ is thus calculated to be 1.46, which is very close to that characterized by the octahedral geometry, $\sqrt{2}$. This finding indicates that there exists such an ionic aggregation as $LaCl_6^{3-}$ complex ion in the melt. Further deduction of the La–La pair distance of 0.518 nm and the existence of octahedra reaches a conclusion that two octahedra are linked with each other through a common Cl atom so as to form a probable associated species, $[La_2Cl_{11}]^{5-}$. It should be stressed that the estimated coordination number of La–Cl pair, 6.20, is an averaged value, meaning that the CN is not fixed at 6 and the distribution of CN should be admitted to be different CN's of 5, 6, 7 and so on, as described before [27].

3.2. XAFS

The extracted XAFS function $k^3\chi(k)$ and radial distribution function $\Phi(R)$ of molten $LaCl_3$, where the latter is sometimes called Fourier transform magnitude |FT|, are shown in Figs. 4 and 5, respectively, together with those of solid $LaCl_3$. The maximum k value used in the Fourier transformation was $54.6\,nm^{-1}$ for the melt data. No corrections, such as the phase shift and backscattering amplitude, were made in the $\Phi(R)$ functions. The oscillation in the $k^3\chi(k)$ function and the peak height in the $\Phi(R)$ function decreases by a rise of temperature or melting. A phase shift to lower k direction by melting was also detected in the $k^3\chi(k)$ function. The first peaks in both $\Phi(R)$ functions are assigned to the nearest La–Cl correlation. In the solid state, there are two peaks over $r = 0.38$–0.50 nm. There is, however, no broad peak around 0.47 nm in the molten state, which has been reported to exist as the La–La correlation [23]. Structural

Table 1
Least-squares fitted structural parameters for molten $LaCl_3$

i–j	n_{ij}	r_{ij} (nm)	$\left\langle \Delta r_{ij}^2 \right\rangle^{1/2}$ (nm)	b_{ij} (nm^2)
La–Cl	6.20	0.282	0.030	4.51E-4
Cl–Cl	7.14	0.412	0.072	2.58E-3
La–La	4.58	0.518	0.080	3.22E-3

Table 2
Structural parameters of La–Cl pair obtained from the XAFS curve fitting in *R*-space

Sample	*i–j*	n_{ij}	r_{ij} (nm)	σ_j^2 (nm^2)	C_3 (nm)	C_4 (nm)
$LaCl_3$ at RT	La–Cl	6.00	0.278	0.0000349	–	–
	La–Cl	3.21	0.305	0.0000895	–	–
$LaCl_3$ at 673 K	La–Cl	8.03	0.279	0.0001534	0.0000220	−0.00019305
$LaCl_3$ at 1173 K	La–Cl	7.12	0.282	0.0002181	0.0006892	0.00068978

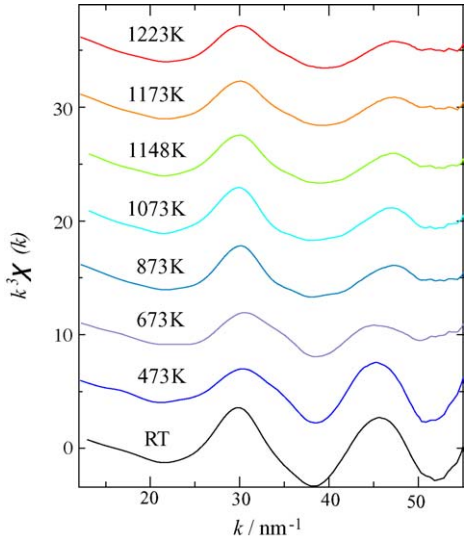

Fig. 4. Extracted XAFS function $k^3\chi(k)$ of molten $LaCl_3$.

parameters of La–Cl pair obtained from the XAFS curve fitting in *R*-space are listed in Table 2. In the curve fitting for solid $LaCl_3$, no third nor fourth cumulant [20] was contained for evaluating anharmonic vibration effects. As can be seen from Table 2, some structural changes seem to occur in $LaCl_3$ from RT to 1173 K since the CN and the interatomic distance of La–Cl pair varied certainly. The first coordination shell

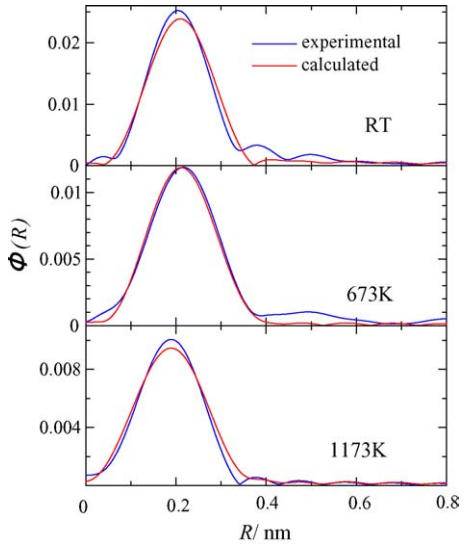

Fig. 5. Radial distribution function $\Phi(R)$ of molten $LaCl_3$.

of solid $LaCl_3$ at RT can be described by two types of short La–Cl correlation at 0.278 nm and long one at 0.305 nm. From detailed investigation of the peak heights and half widths in Fig. 5, the local structure of solid $LaCl_3$ is found to be different from that at RT, giving decreases of coordination number ($6.00 + 3.21 \rightarrow 8.03$) and interatomic distance (0.278 nm, 0.305 nm → 0.279 nm), implying the existence of another stable state in solid $LaCl_3$ before melting at 1150 K [28]. The decrease in coordination number for La–Cl pair from RT to 1173 K is thought to be due to the increase in molar volume and to be well interpreted by that on melting, for instance, 19.1% [29]. As pointed out in introduction section, Wasse and Salmon [10,11] reported that the CN of the first La–Cl correlation in molten $LaCl_3$ was 8.2. In contrast, the corresponding CN in solid $LaCl_3$ was 9, as described in [26]. This small difference in CN from 9 (solid) to 8.2 (melt) would be rather difficult to be explained from the large expansion in molar volume on melting, 19.1% [29] since the change of CN from 6 (solid) to 4.0–4.5 (melt) on melting of several alkali halides corresponded to the volume change of about 20%.

There was also found a discrepancy between the results of XRD and XAFS concerning the coordination number of La–Cl pair. However, this would be almost within the permissible range by taking into account the statistical errors estimated in XRD and XAFS experiments.

4. Conclusions

The results of molten $LaCl_3$ indicate that there is such an ionic aggregation as $LaCl_6^{3-}$ complex ion in the melt, and two octahedra are linked with each other through a common Cl atom to form a probable associated species $[La_2Cl_{11}]^{5-}$. It is also found from this work that some structural changes seem to occur in $LaCl_3$ from RT to 1173 K, but XAFS experiments were performed in the very limited range of *k* due to the restriction on machine time and so on. Further accumulation of the data by diffraction and XAFS is desired.

Acknowledgements

The synchrotron radiation XAFS experiments were performed at BL-7C beam line in High Energy Accelerator Research Organization (KEK) at Tsukuba with the approval of KEK-PF (Prop. Nos. 2002G281 and 2003G084). The XAFS facilities and computer time made available to us from KEK are gratefully acknowledged.

References

[1] N. Ohtori, in: Y. Shiokawa, H. Yamana (Eds.), Proceedings of the Specialists' Meeting on the Chemistry and Technology of Actinide Elements 2003, RRI Kyoto Univ., 2004, pp. 33–53, KUR Report (KURRI-KR-107).
[2] T. Nagai, ibid., pp. 129–144.
[3] G.N. Papatheodorou, Inorg. Nucl. Chem. Lett. 11 (1975) 483.
[4] G.N. Papatheodorou, J. Chem. Phys. 66 (1977) 2893.
[5] G.M. Photiadis, B. Børrensen, G.N. Papatheodorou, J. Chem. Soc., Faraday Trans. 94 (1998) 2605.
[6] J. Mochinaga, Y. Iwadate, K. Fukushima, Mater. Sci. Forum 73–75 (1991) 147.
[7] M.-L. Saboungi, D.L. Price, C. Scamehorn, M.P. Tosi, Europhys. Lett. 15 (1991) 283.
[8] J. Mochinaga, M. Ikeda, K. Igarashi, K. Fukushima, Y. Iwadate, J. Alloys Compd. 193 (1993) 36.
[9] Y. Okamoto, H. Hayashi, T. Ogawa, Jpn. J. Appl. Phys. 38 (1999) 156.
[10] J.C. Wasse, P.S. Salmon, Phys. B 241–243 (1998) 967.
[11] J.C. Wasse, P.S. Salmon, J. Phys.: Condens. Matter 11 (1999) 1381.
[12] F. Hutchinson, A.J. Rowley, M.K. Walters, M. Wilson, P.A. Madden, J.C. Wasse, P.S. Salmon, J. Chem. Phys. 11 (1999) 2028.
[13] F. Hutchinson, M. Wilson, P.A. Madden, Mol. Phys. 99 (2001) 811.
[14] J.A. lbers, W.C. Hamilton (Eds.), International Tables for X-ray Crystallography, vol. 4, Kynoch, Birmingham, 1974, p. 99.
[15] F. Hajdu, Acta Cryst. Sec. A 27 (1971) 73.
[16] H. Matsuura, A.K. Adya, D.T. Bowron, J. Synchr. Rad. 8 (2001) 779.
[17] J.A. Solera, J. Garcia, M.G. Proietti, Phys. Rev. B 51 (1995) 2678.
[18] T. Ressler, J. Phys. IV 7 (1997) C2–C269.
[19] S.I. Zabinsky, J.J. Rehr, A. Aukudinov, R.C. Albers, M.J. Eller, Phys. Rev. B 52 (1995) 2995.
[20] G. Bunker, Nucl. Instrum. Meth. Phys. Res. 207 (1983) 437.
[21] Y. Okamoto, M. Akabori, H. Motohashi, H. Shiwaku, T. Ogawa, J. Synchr. Rad. 8 (2001) 1191.
[22] Y. Okamoto, M. Akabori, H. Motohashi, A. Itoh, T. Ogawa, Nucl. Instrum. Meth. Phys. Res. A 487 (2002) 605.
[23] Y. Okamoto, H. Shiwaku, T. Yaita, H. Narita, H. Tanida, J. Mol. Struct. 641 (2002) 71.
[24] A.H. Narten, J. Chem. Phys. 56 (1972) 1905.
[25] R.D. Shannon, Acta Cryst. Sect. A 32 (1976) 751.
[26] R.W.G. Wyckoff, Crystal Structures, vol. 2, Interscience, New York, 1964, p. 78.
[27] Y. Iwadate, H. Yamoto, K. Fukushima, R. Takagi, J. Mol. Liq. 83 (1999) 41.
[28] K. Igarashi, J. Mochinaga, Z. Naturforsch. 42a (1987) 777.
[29] K. Igarashi, J. Mochinaga, Z. Naturforsch. 42a (1987) 690.